Proceedings of the ASME 2010 3rd Joint US-European Fluids Engineering Summer Meeting and 8th International Conference on Nanochannels, Microchannels, and Minichannels
FEDSM-ICNMM2010
August 1-5, 2010, Montreal, Canada

FEDSM-ICNMM2010-30504

NUMERICAL AND EXPERIMENTAL INVESTIGATIONS OF CAVITATING FLOW IN A VERTICAL MULTI-HOLE INJECTOR NOZZLE

HE Zhixia
School of Energy and Power Engineering,
Jiangsu University
Zhenjiang, Jiangsu Province, China
Email: zxhe@ujs.edu.cn

BAI Jing
School of Energy and Power Engineering,
Jiangsu University
Zhenjiang, Jiangsu Province, China
Email: perking1984@yahoo.cn

WANG Qian
School of Energy and Power Engineering,
Jiangsu University
Zhenjiang, Jiangsu Province, China
Email: qwang@ujs.edu.cn

MU Qingmu
School of Energy and Power Engineering,
Jiangsu University
Zhenjiang, Jiangsu Province, China
Email: 1982qingmu@163.com

HUANG Yunlong
School of Energy and Power Engineering,
Jiangsu University
Zhenjiang, Jiangsu Province, China
Email: huangyunlongujs@163.com

ABSTRACT

The presence of cavitation and turbulence in a diesel injector nozzle has significant effect on the subsequent spray characteristics. However, the mechanism of the cavitating flow and its effect on the subsequent spray is unclear because of the complexities of the nozzle flow, such as the cavitation phenomena and turbulence. A flow visualization experiment system with a transparent scaled-up vertical multi-hole injector nozzle tip was setup for getting the experimental data to make a comparison to validate the calculated results from the three dimensional numerical simulation of cavitating flow in the nozzle with mixture multi-phase cavitating flow model and good qualitative agreement was seen between the two sets of data. The critical conditions for cavitation inception were derived as well as the relationship between the discharge coefficient and non-dimensional cavitation parameter. After wards, the testified numerical models were used to analyze the effects of injection pressure, back pressure, cavitation parameter, Reynolds number, injector needle lift and needle eccentricity on the cavitating flow inside the nozzle. Combined with visual experimental results, numerical simulation results can clearly reveal the three-dimensional nature of the nozzle flow and the location and shape of the cavitation induced vapor distribution, which can help understand the nozzle flow better and eventually put forward the optimization ideas of diesel injectors.

INTRODUCTION

The injector nozzle is one of the most important parts of a Diesel engine. For a long time, the mechanism of atomization of the fuel sprays through the injector nozzle is generally thought to be aerodynamic atomization theory [1]. However, the further theoretical and experimental studies[2-5] for the injection spray show that the fuel sprays atomization without a fully break-up processes can be divided into two main processes, primary and secondary break-up. The former takes place in the region very close to the nozzle. It is not only determined by the interaction between the liquid and gaseous phases but also by internal nozzle phenomena like turbulence and cavitation. The latter occurs further downstream in the spray due to aerodynamic interaction processes and which is largely independent of the nozzle type. Cavitation patterns extend from their starting point around the nozzle orifice inlet to the exit, where they influence the formation of the emerging spray and enhance the atomization of it. The improved spray development is believed to lead to a more complete combustion process, lower fuel consumption, and reduced exhaust gas and particulate emissions. However, cavitation can also decrease the flow efficiency (discharge coefficient) due to its affect on

the exiting jet. Also imploding cavitation bubbles inside the orifice can cause material erosion and then decrease the life and performance of the injector. Thus, a thorough understanding of the internal flow physics inside the nozzle is fundamental for predicting spray characteristics and sprays atomization behavior, which are decisive for engine performance and pollutant formation and is also very important for more efficient nozzle designs.

Unfortunately, the physics of diesel injector nozzle flow is poorly understood for the complexities of the nozzle flow, such as the cavitation phenomena and turbulence. The nozzles are extremely small, typically about a millimeter long and a fraction of a millimeter in diameter, the flow through the holes moves at very high speeds, on the order of several hundred meters per second, the flow is transient with injection duration on the order of a few milliseconds and the internal flow is two-phase and highly turbulent, with a Reynolds number on the order of 50000. All these make it quite difficult to directly observe the cavitating flow inside the real size nozzle holes by visualization experiments. Thus, for a long time the emphasis has been put on the numerical simulations.

In this research, a flow visualization experiment system with a transparent scaled-up diesel vertical multi-hole injector nozzle tip was setup for getting the experimental data to make a comparison to validate the calculated results from 3d numerical model of cavitating flow in the nozzle. As we know, cavitation inception has been a research focus in this area and it can be caused by “geometrical” and “dynamic” factors [6]. Geometrical parameters include the type of orifice (valve covered orifice (VCO) or minisac), orifice inlet curvature, orifice length, ratio of inlet to outlet orifice diameter. Dynamic parameters include the injection pressure, injector needle lift and needle eccentricity. Thus, after we have finished analyzing the effect of the nozzle geometrical parameters on the cavitating flow in a nozzle [7, 8], we put focus on dynamic parameters and in this paper the modified and testified numerical models of cavitating flow in nozzles were then used to analyze the influence of the injection pressure, back pressure, injector needle lift and needle eccentricity on the cavitating flow in the nozzle.

THEORETICAL ANALYSES

Cavitation refers to the formation of bubbles in a liquid flow leading to a two-phase mixture of liquid and vapor/gas, when the local pressure drops below the vapor pressure of the fluid. Fundamentally, the liquid to vapor transition can occur by heating the fluid at a constant pressure, known as boiling, or by decreasing the pressure at a constant temperature, which is known as cavitation. For most applications, cavitation is hypothesized to occur as soon as the local pressure drops below the vapor pressure of the fluid at the specified temperature. In a diesel injector nozzle, due to the abrupt change in flow direction, the boundary layer tends to separate from the wall at the inlet section. As a consequence, a recirculation phenomenon appears in this zone, accompanied by a pressure fall due to the acceleration of the fluid. As mentioned above, when the static pressure falls under vapor pressure of the working fluid, cavitation will occur.

There are two important non-dimensional parameters for description of the cavitating flow characteristics in nozzle holes, which are discharge coefficient and cavitation number.

The discharge coefficient of a nozzle can be obtained by combining the Bernoulli equation and the mass conservation equation

$$C_d = \frac{\dot{m}}{A\sqrt{2\rho_l(p_i - p_b)}}, \qquad (1)$$

where $\dot{m}$ is actual mass flow rate, A is the cross-section area of a nozzle hole, ρ_l represents the liquid density, p_i is the upstream nozzle pressure (injection pressure) and p_b the orifice outlet pressure.

The cavitation parameter is usually defined as:

$$K = \frac{p_i - p_v}{p_i - p_b}, \qquad (2)$$

where p_v is the vapor pressure.

For cavitating nozzles, the critical cavitation parameter is defined as K_{crit}, corresponding to the pressure drop at which cavitation starts in the injector orifice, which means cavitation will not occur unless the cavitation parameter that corresponds to these pressure conditions is lower than the critical value (K_{crit})[8].

EXPERIMENTAL SETUP

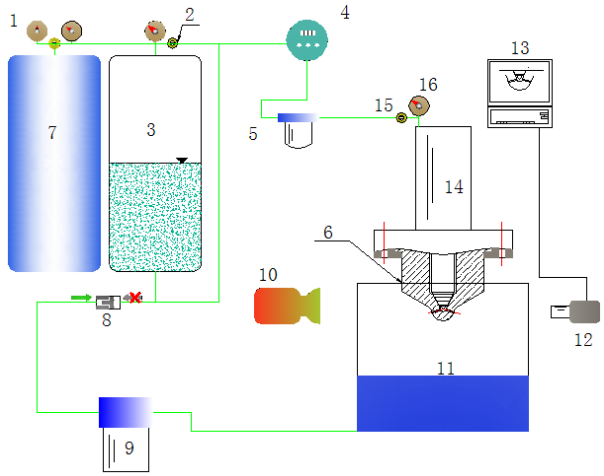

1.Pressure Regulator 2.Release Valve 3.Fuel tank 4.Flow rate meter 5.Filter 6.Transparent nozzle tip 7.Nitrogen gas 8.Control Valve 9.Pump 10.High power white LED light 11.Catch tank 12. HCCD Camera 13.Image grabber 14.Needle and nozzle valve 15.Control valve 16.Pressure gauge

Fig.1. Schematics of flow visualization system

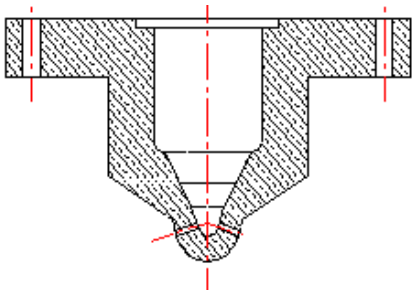

Fig.2 Transparent nozzle tip

A schematic diagram of the flow visualization system used for the current work is shown in Fig.1. The vertical four-hole nozzle tip was made of transparent acrylic and is ten times larger in size than an actual nozzle, as shown in Fig.2. The diameter of the nozzle hole is 3.2mm and the length of it is 10mm. A fuel tank pressurized with nitrogen gas was used to supply a fuel to the test nozzle, and a flow rate meter (LWGY-15) was installed to measure the instant flow rate. The injection pressure of each experimental case was determined by a pressure gauge located at the entrance of the nozzle.

During fuel injection, the nozzle was illuminated with a high power white LED light (100W) and the cavitation condition in the nozzle was photographed with a high speed digital camera (MotionPro -TM10000) with a Nikon Nikkor lens (AF Micro 60mm f/2.8D). All captured images were digitally stored in a computer using image grabber and processing software.

THE MATHEMATIC MODEL

The multi-dimensional mathematic model of cavitating nozzles is set up on the basis of single-bubble collapse model developed by Lord Rayleigh [9]. An order of magnitude analysis [10] indicates that, for the present nozzles flows, relative motion of the two phases can be neglected, so we consider the vapor-liquid flow a homogeneous bubble-liquid mixture (The fluid is homogeneously mixed on the sub-grid scale). There is no differentiation between phases, so the basic equations of continuity and momentum are the same as those in single-phase flow except that the density and dynamic viscosity in nozzles cavitating flows use the mixture density ρ and the mixture dynamic viscosity μ

$$\rho = \alpha_1\rho_1 + \alpha\rho_v \tag{3}$$

$$\mu = \alpha_1\mu_1 + \alpha\mu_v \tag{4}$$

Where α is the volume fraction of vapor, α_1 is the volume fraction of liquid. The mixture model allows the phases to be interpenetrating. α and α_1 for a control volume can therefore be equal to any value between 0 and 1, depending on the space occupied by the vapor phase and the liquid phase. The subscripts l and v stand for the properties of pure liquid and pure vapor which are assumed to be constant.

The vapor in cavitation zone is assumed to consist of mini spherical bubbles which are neither created nor destroyed. When the radius of the bubble is r, α can be calculated as

$$\alpha = \frac{V_v}{V_l + V_v} = \frac{n_0 \cdot 4\pi r^3/3}{1 + n_0 \cdot 4\pi r^3/3}, \tag{5}$$

where n_0 is defined as the population of bubbles per unit volume of pure liquid. It is known in advance.

Thus, assuming an incompressible liquid, the basic governing equations of the mathematic model for the three dimensional cavitating two-phase turbulent flow in a nozzle are as follows [7,11,12]

(1) The continuity equation

$$\frac{\partial\rho}{\partial t} + \nabla(\rho\mathbf{v}) = 0 \tag{6}$$

(2) The momentum equation

$$\frac{\partial(\rho\mathbf{v})}{\partial t} + \nabla(\rho\mathbf{v}\mathbf{v}) = -\nabla p + \nabla\left[\mu\left(\nabla\mathbf{v} + \nabla\mathbf{v}^{\Gamma}\right)\right] + \rho\mathbf{g} + \mathbf{F} \tag{7}$$

(3) The volume fraction equation

$$\frac{\partial\alpha_1}{\partial t} + \nabla(\alpha_1\mathbf{v}) = \frac{\rho_1}{\rho}\frac{n_0}{(1+n_0\phi)^2}\frac{\mathrm{d}\phi}{\mathrm{d}t} + \frac{\alpha\rho_v}{\rho}\frac{d\rho_v}{\mathrm{d}t} \tag{8}$$

(4) For the process of the single bubble growth and collapse, the Rayleigh-Plesset equation is as follows [10]

$$r\frac{\mathrm{d}^2 r}{\mathrm{d}t^2} + \frac{3}{2}\left(\frac{\mathrm{d}r}{\mathrm{d}t}\right)^2 = \frac{p_b - p}{\rho_l} - \frac{2\sigma}{\rho_l r} - 4\frac{\mu_l}{\rho_l r}\frac{\mathrm{d}r}{\mathrm{d}t} \tag{9}$$

(5) The k-ε equations

$$\frac{\partial}{\partial t}(\rho k) + \nabla\cdot(\rho\mathbf{v}k) = \nabla\cdot\left(\frac{\mu_t}{\sigma_k}\nabla k\right) + G_k - \rho\varepsilon \tag{10}$$

$$\frac{\partial}{\partial t}(\rho\varepsilon) + \nabla\cdot(\rho\mathbf{v}\varepsilon) = \nabla\cdot\left(\frac{\mu_t}{\sigma_\varepsilon}\nabla\varepsilon\right) + \frac{\varepsilon}{k}\left(C_{1\varepsilon}G_k - C_{2\varepsilon}\rho\varepsilon\right) \tag{11}$$

$$\mu_t = \rho C_\mu\frac{k^2}{\varepsilon} \tag{12}$$

$$G_k = \eta_t\nabla\mathbf{v}\left[\nabla\mathbf{v} + (\nabla\mathbf{v})^{\Gamma}\right] \tag{13}$$

(6) The logarithmic law conditions for the wall boundaries

$$u^+ = \frac{u}{u_\tau} = \frac{1}{\kappa}\ln\left(\frac{yu_\tau}{\upsilon}\right) = \frac{1}{\kappa}\ln\left(y^+\right) + B \tag{14}$$

$$k = \frac{(u^*)}{(C_t)^{1/2}}, \quad \varepsilon = \frac{(u^*)^3}{\kappa y} \tag{15}$$

$C_{1\varepsilon}$=1.44, $C_{2\varepsilon}$=1.92, σ_k=1.0, σ_ε=1.3, C_μ=0.09, κ=0.42, B=5.44

Where $\mathbf{v}$ is velocity vector, p is pressure, F is body force, t is time, k is turbulence kinetic energy, ε is dissipation rate, p_b is pressure within the bubble, σ is surface tension of the fluid, y is

distance from the wall surface, y^+ is dimensionless distance from the wall surface, u^+ is velocity component tangential to the wall, u_τ is friction velocity constructed from the wall stress, υ is kinetic viscosity.

THREE-DIMENSION NUMERICAL SIMULATIONS

The three dimensional numerical simulations of the two-phase flow in the holes of a vertical multi-hole nozzle were carried out. The nozzle geometrical model for simulations is the same with the experimental nozzle model.

Computational Domain and Grid

The vertical four-hole nozzle has the same angle between every injection holes axis and the needle seat axis, and therefore all the four holes are set up for proportional spacing along circumference and the calculations are performed to the 1/4 of the nozzle except when needle is eccentric. Thus, only a quarter of the nozzle was simulated for calculation. The three-dimensional structural computational grid formed by the domain-subdividing and matching method is shown in Fig.3. A local mesh refinement scheme was used to the holes of the nozzle. Due to the presence of cavitation in the nozzle hole, the pressure at the exit may vary greatly from the surrounding atmospheric pressure. When the atmospheric pressure is used for the pressure exit boundary conditions of nozzle, the accuracy of the calculation results may be affected. Thus, in this paper, a region, corresponding to the computational area outside the nozzle holes, was provided at the hole exit and the computational zone was built as Fig.3. At this time, the atmospheric pressure applied at the exit will be much close to the practical cases. And the effects of the hole exit boundary conditions on the flow inside the hole will also decrease.

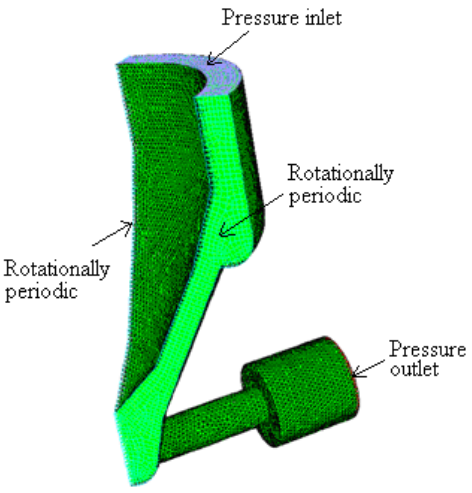

Fig.3. Computational domain and grid

Boundary Conditions

The boundary conditions for the nozzle computation are listed in the following table 1.

Table1. Boundary conditions of the nozzle

Boundaries	Velocity	Pressure (MPa)	$k-\varepsilon$
Pressure inlet	$\partial u/\partial n=0$	$p=0.15\sim1.5$	$I=0.16\times(Re)^{-1/8}$ $l=0.07D$
Pressure outlet	$\partial u/\partial n=0$	$p=0.1$	$I=0.16\times(Re)^{-1/8}$ $l=0.07D$
Wall	$u=0$	$\partial p/\partial n=0$	$k=(u^*)^2/(C_t)^{1/2}$ $\varepsilon=(u^*)^3/ky$
Rotationally periodic	——	$\partial p/\partial n=0$	——

At inlet and outlet sections, pressure boundary conditions were applied. For the wall, the boundary conditions were defined as the impermeability and no-slip for the velocity. A standard wall-function was also used for the turbulence modeling. The two sections formed when a quarter of nozzle is cut out for computation were both treated as the rotationally periodic conditions through which there is no pressure reduction.

Discretization and Solution of Equations

The discretization method of the equations was based on the finite volume approach and the coupling of velocity and pressure was achieved using a SIMPLEC algorithm. The convective term of Eq.(8) was approximated with a hybrid method which combines central differencing and upwind differencing algorithms

$$\alpha_c=\beta\alpha_u+(1-\beta)\alpha_d \tag{16}$$

where the weighting factor β was set to be 0.72 in this study. The spatial discretization scheme for convective term of the momentum equations used here was the first order upwind differencing algorithms and the others used the second order central differencing algorithms. The time was implicitly discretized.

The calculations were performed by first computing the volume fraction equation (Eq.(8)) for the new time step, and then using the new volume fraction of vapor and liquid, i.e., the new mixture density, to calculate the momentum equations coupled with the continuity equations of the flow via an iterative process.

During the specific calculation progress, the initial flow field of single-phase convergence may be acquired quickly without solution of the volume fraction equations first. Subsequently, the volume fraction equations were added to activate the mixture multiphase model and perform the

calculation of the mixture phases. The calculation program is showed in Fig.4.

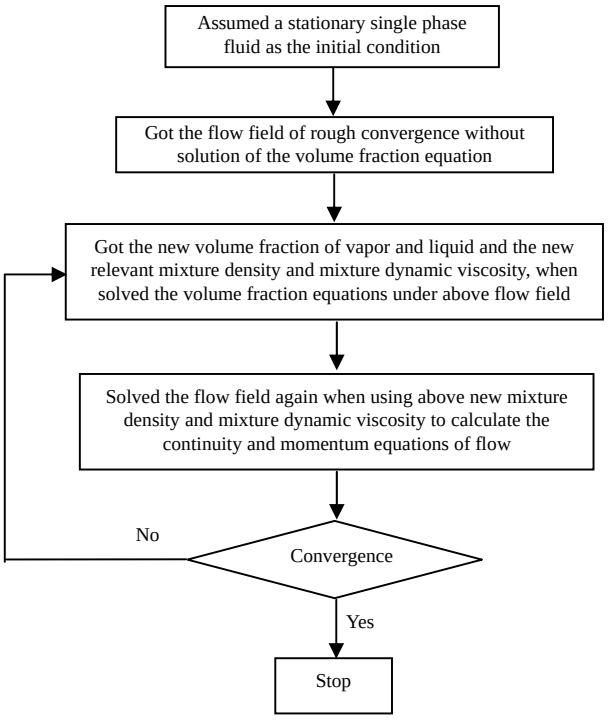

Fig.4. Calculation Program

RESULTS AND DISCUSSIONS

Comparisons of Cavitating Flow between the Numerical Simulations and Experiments

In the above descriptions of the mathematical models of cavitating flow in the nozzle, the population of bubbles per unit volume of pure liquid n_0 is a very important parameter given in advance for numerical simulations. In this work, based on the nozzle cavitation and fuel flow images acquired from the flow visualization system, comparisons, analyses and lots of trial calculations were conducted and then the initial cavitation bubble number density has been set to $n_0 = 1.5\times10^{11}$. Then the calculated results obtained with the cavitation model with $n_0 = 1.5\times10^{11}$ are compared in Fig.5 with the results visualized in experiments conducted with a tenfold scaled-up model. It is clear that the cavitation is formed at the top of the hole and proceeded downstream and the cavitation inception occurs under the injection pressure of about 0.2MPa.

In order to know about the three dimensional cavitation structure, the photos were taken from two different views, side view and top view, shown in Fig.6. It can be seen that the calculated results agree with the experimental results both from side view and top view quite well.

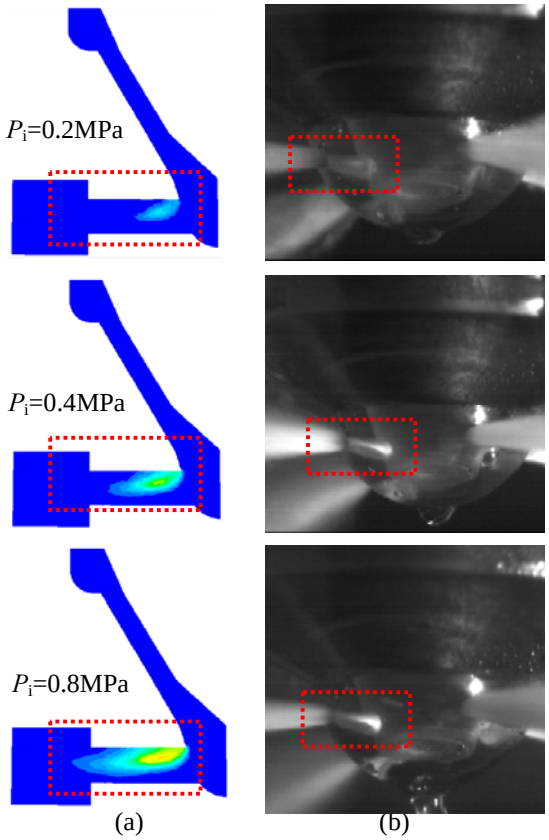

Fig.5.comparison of cavitation from numerical simulations (a) and experiments (b) under different injection pressures

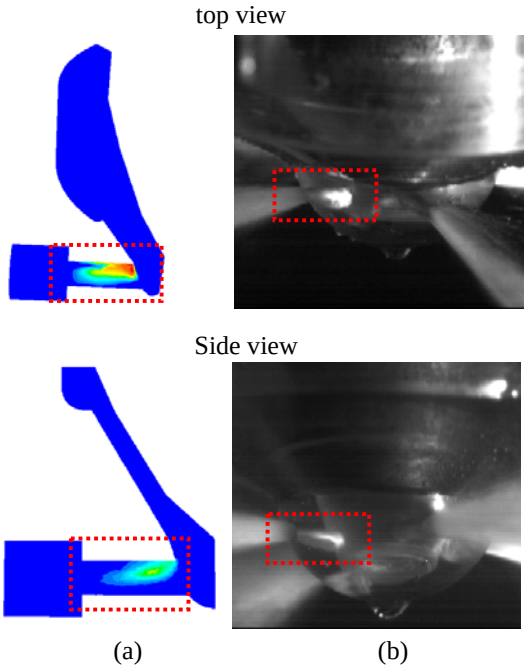

Fig.6.comparison of cavitation from numerical simulations (a) and experiments (b) from different views (p_i=0.3MPa)

Analyses of Cavitating Flow with Different Injection Pressures and Back Pressures

VCO (Valve Closed Orifice) nozzles are quite typical nozzles used commonly in diesel engines, so the above modified and testified numerical models for cavitating flow in nozzles were used to analyze the cavitating flow in the VCO nozzle with a needle lift of 0.3mm.

Figure 7 shows the vapor fraction distribution inside the nozzle hole when the injection pressure varies from 100MPa to 140MPa, 50MPa, 12MPa, 5MPa and 3MPa while keeping back pressure to a constant value of 0.1MPa. This results in cavitation parameters ranging from 1.0007 to 1.034 and Reynolds numbers from 126080 to 18560. Although the injection pressure varies quite larger from 3MPa to 140MPa, the back pressure is only 0.1MPa, relatively smaller and subsequently the non-dimensional cavitation parameters change less and are all very close to 1.0. Thus, for all above different injection pressure cases, the cavitation can extend to the nozzle exit closely along the wall. It can be concluded that The cavitation depends mainly on cavitation parameter *K*, but not injection pressure. It can be also seen from Fig.7 that cavitation separates from the wall near the nozzle exit with the decrease of the injection pressure.

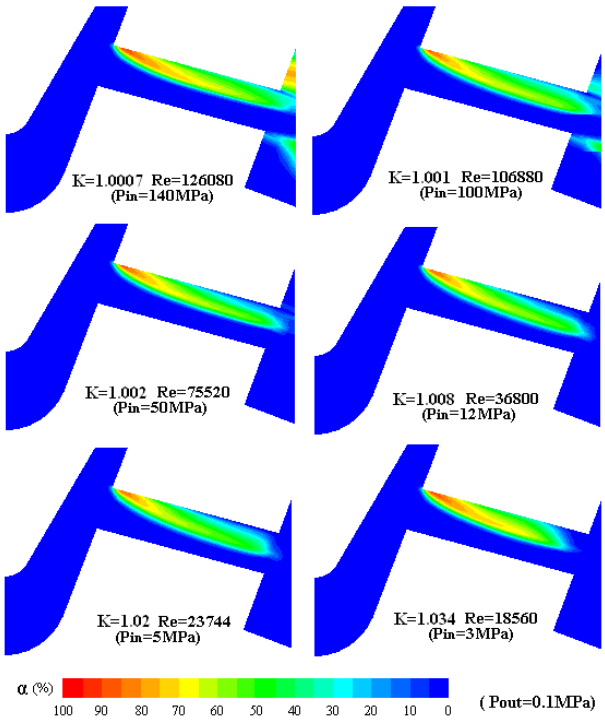

Fig.7. The contour of volume fraction of vapor with different injection pressures（p_{out}=0.1MPa）

Figure 8 shows the numerical simulation results when the back pressure increases from 0.1MPa to 3.0MPa at a constant injection pressure of 12MPa. It can be seen that increase of the back pressure while keeping constant injection pressure results in largely increase of cavitation parameter and obvious decrease of the extent of the cavitation, especially nearly vanishing of the cavitation for the back pressure of 3MPa and cavitation parameter *K* of 1.33. Thus, we can conclude that the critical cavitation parameter K_{crit} is about 1.33 for the nozzle and when *K* is smaller than 1.33, the cavitation phenomenon will occur. We also notice the variation of the cavitation parameter even while keeping approximately the same flow rate through the nozzle, i.e. almost the same Reynolds number.

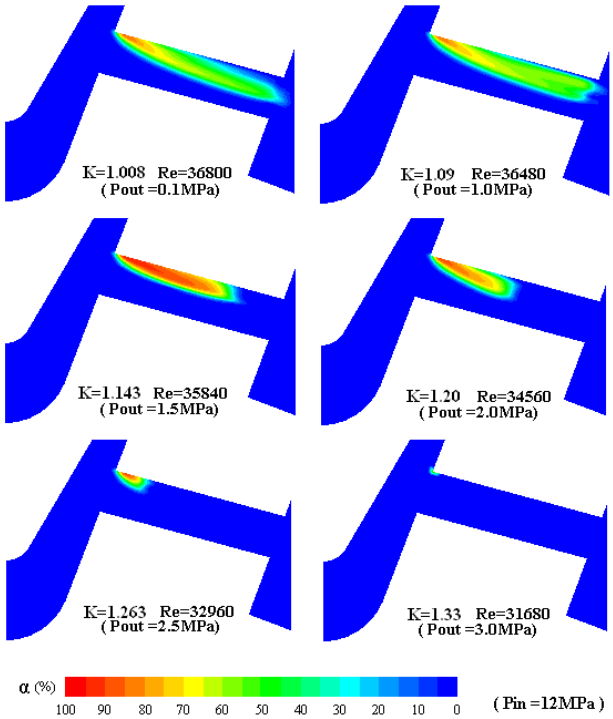

Fig.8. The contour of volume fraction of vapor with different back pressures（p_{in}=12MPa）

In order to investigate the effect of the Reynolds number, both the injection and back pressure have been varied simultaneously while keeping the cavitation parameter a constant value of 1.15. The simulation results of the vapor fraction distributions i.e. cavitation distributions are shown in Fig.9. From Fig.9, although the injection pressure, back pressure and the pressure difference between them are different and the average velocity inside the hole and the corresponding Reynolds numbers are also varied, the thickness and extent of the cavitation are very similar because of the same cavitation parameters. All these indicate that there is no significant variation in the hole flow structure with increase of Reynolds number in the range of values investigated here. The result is consistent with the observations of Arcoumanis C et al. [13]. That is, with the increase of the Reynolds number, the images of cavitating flow obtained from experiment are similar at

constant cavitation parameter. The flow structures formed inside the nozzle hole have much little difference and the flow regimes are also nearly identical. The numerical simulation in this paper verified again that the cavitation parameter is the most important parameter affecting the flow structure inside the injection hole.

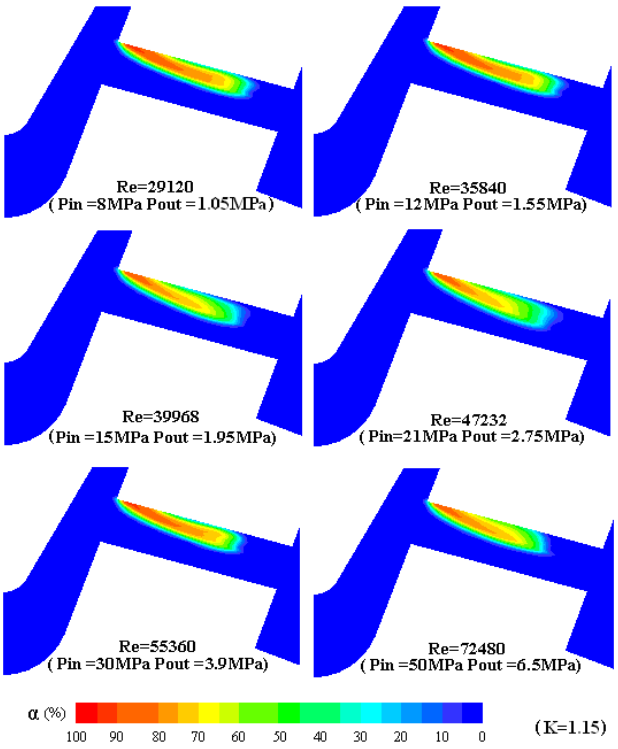

Fig.9. The contour of volume fraction of vapor with the same cavitation parameter（K=1.15）

Analyses of the Cavitating Flow in the Nozzle Holes with Needle Eccentricity

Ideally, the needle and its seat have the same axis. The flow between them should be totally symmetrical and the flow rate between the various holes should also be equal wholly. However, the flow in realistic nozzles is often asymmetric for different factors such as the hole size, hole roughness, hole entrance shape and actual position of the needle relative to the axis of symmetry of the nozzle. Especially for the multi-hole VCO nozzle, the phenomenon is more representative and the flow inside the nozzle hole will be absolutely different from that in the symmetric nozzle hole. The flow rate between the various holes is different. At the same time, the small, uncontrolled asymmetries will have a strong effect on the distribution of the cavitation in the nozzle hole and create complex features of the flow field that are not found in symmetric nozzles. Therefore, the study of the cavitating flow in the asymmetric nozzle will be more realistic.

The numerical simulation of cavitating flow in the nozzle with the needle eccentricity is conducted for constant needle lifts of 0.1mm and 0.3mm. The schematic of needle eccentricity is showed in Fig.10. When the needle lift correspond to 0.1mm and 0.3mm respectively, the needle is placed at 0.031mm and 0.1mm from the nozzle axis towards hole 3 respectively. The computational grid for a needle lift of 0.3mm is showed in Fig.11. It consists of 134180 cells. All the numerical methods are same as that of the above model except for no rotationally periodic boundaries.

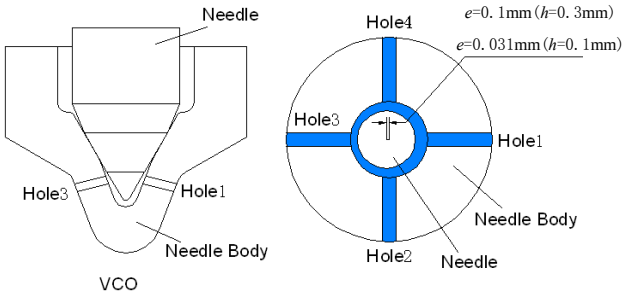

Fig.10.The schematic of needle eccentricity

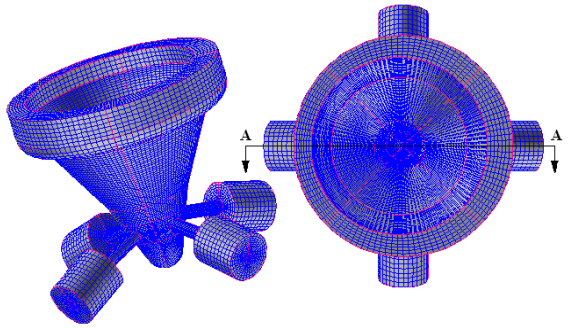

Fig.11.The computational grid under eccentric needle condition

The calculated velocity distribution in the vertical cross section A-A is showed in Fig.12 under two different needle lifts. Because the needle is placed from the nozzle axis towards hole 3, the annular cross-sectional area towards hole 1 is larger and the fluid can not all been delivered through this hole and parts of the fluid flow below the needle tip towards hole 3. That results in a larger flow rate through this hole which is showed from the individual hole flow rate calculated in Fig.13. The x-coordinate stands for the hole index and the y-coordinate stands for the percentage of relative variation of volumetric flow rate of every hole from the mean value with concentric needle. The figure presents that this variation of all the holes is larger for the low lift case. This phenomenon is also seen from the fig.12. The flow from below the needle tip to hole 3 is stronger and the velocity distribution in hole 3 is more uniform for the low lift case than for the high lift case.

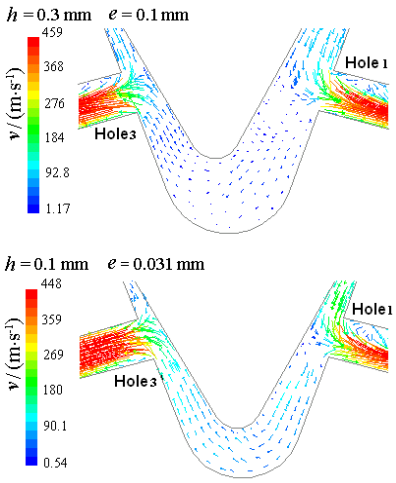

Fig.12.The vector of velocity under eccentric needle condition

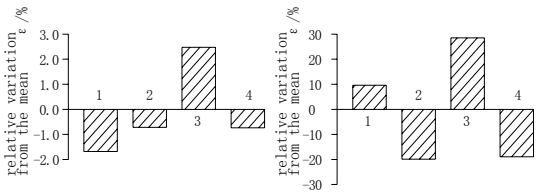

Fig.13.The percentage of relative variation of volumetric flow rate of every hole from the mean value with concentric needle

Figure 14 presents the distribution of the vapor volume fraction and pressure. For the high lift case the local pressure minimum occurs at the top corner of nozzle hole3, for the low needle lift case this minimum is formed at the bottom corner since most of the fluid is delivered to the hole from the flow below the needle tip. Accordingly, the cavitation extends to the hole exit along the top of the hole for the high needle lift case while it occurs at the bottom of the hole for the low lift case.

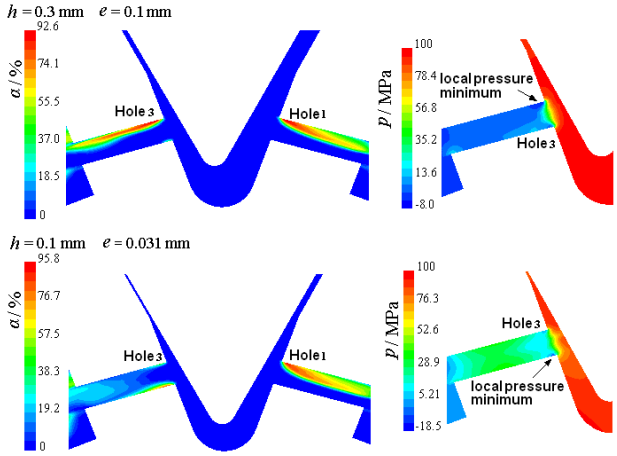

Fig.14.The contour of volume fraction of vapor and pressure under eccentric needle condition

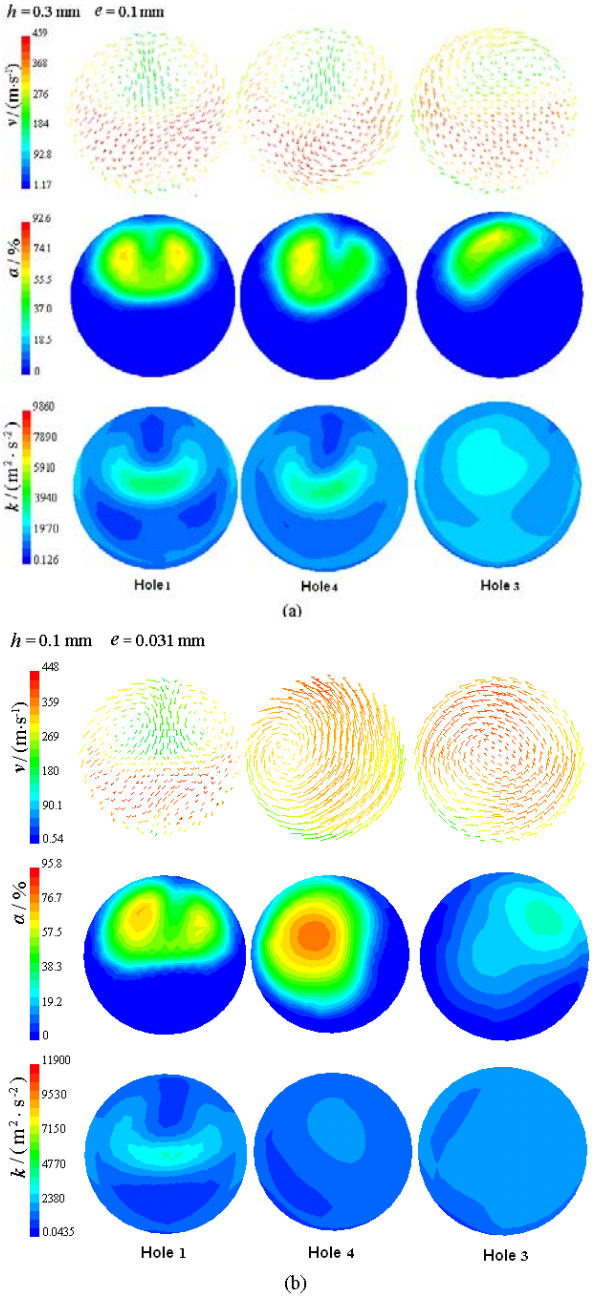

Fig.15.The contour of velocity, volume fraction of vapor and turbulent kinetic energy for hole exit with different nozzle holes under eccentric needle condition

Figure 15a and figure 15b show the calculated velocity, vapor volume fraction and turbulent kinetic energy distributions in cross sections at the exit of every hole for the high and low needle lifts, respectively. The calculation results of hole 2 is not showed because hole 2 is identical to hole 4. These results show that the vapor volume fraction distributions are varied at each hole exit and the cavitation is more severe for

the low needle lift case. With the increase of the needle lift, the cavitation tends from the center of all the holes to be skewed toward the top of the hole. The velocity distributions present that the swirl motion generated by the off-center needle position is transferred inside the nozzle holes and persists up to their exit. Especially, the velocity profile at hole 4, as well as hole 2, has a strong swirl component for the low needle lift. It is thought that this strong swirl flow and the associated centrifugal forces contribute to the formation of hollow-cone spray under certain conditions whose image reported in the literature [14]. It can also be seen that the turbulent kinetic energy distributions are different seriously at each hole exit and the corresponding turbulent kinetic energy will be larger when the swirl motion is stronger and the cavitation is heavier. It is thus believed that it is the heavy disturbances at the nozzle hole exit that accelerate the atomization of the injection fluid. All the calculated results show the effect of needle eccentricity is much more remarkable for the low needle lift case.

CONCLUSIONS

Although the cavitation in the fuel injection system has bad effect on the machinery parts, it is advantageous to the break-up process of spray. In the present research, a visualization test rig with a transparent scaled-up vertical multi-hole diesel injector nozzle tip was setup for getting the experimental data to make a comparison to validate the calculated results from 3d numerical model of cavitating flow in the nozzle. Combined with the visualization experiment research, the three-dimensional numerical simulation of the cavitating flow in the holes of a vertical multi-hole nozzle using the mixture multiphase cavitating model clearly reveals the three-dimensional nature of the nozzle flow and the location and shape of the cavitation induced vapor distribution that finally leads to the formation of two distinct cavitation zones at the nozzle hole exit.

The cavitation inception is caused not only by geometrical factors but also by dynamic factors, such as injection pressure, injector needle lift and needle eccentricity. From numerical simulation results, it is concluded that the non-dimensional cavitation parameter is quite effective for representing the cavitation development but not the injection pressure or back injection. The numerical simulation results for needle eccentricity present that the needle eccentricity creates a swirling motion inside the sac volume which is transferred into the holes, giving rise to different flow patterns at their exits. Cavitation mainly initiates at the bottom corner nearer to the needle hole at low lifts while at the top corner at high lifts. There is more obvious effect of needle eccentricity on the flow in the hole for the low lift case. All the analysis show that it is the presence of reverse flow fields with low pressure and strongly affect the flow characteristics at the nozzle hole exit.

ACKNOWLEDGMENTS

This research was supported by the *National Natural Science Foundation of China* (No. 50806030) and *Postdoctoral Science Foundation of China* (No. 20090451170)\

REFERENCES

[1] Amo YuKo, 1998. “The effect of the cavitation in the holes of injection nozzles on the fuel sprays atomization”. *Foreign Diesel Locomotive*, 338(8), pp.23-29.

[2] Chaves H., Knapp M., 1995. “Experimental study of cavitation in the nozzle hole of diesel injectors using transparent nozzles”. *SAE Paper 950290*, pp.199-211.

[3] Schmidt D. P., Corradini M. L., 1997. “Analytical prediction of the exit flow of cavitating orifices”. *Atomization and Sprays*, 7(6), pp.54-65.

[4] Yan C.L., Aggarwal S. K., 2006. “A High-Pressure Droplet Model for Spray Simulations”, *Transactions of the ASME. Journal of Engineering for Gas Turbines and Power*, 128(3), pp.482-492.

[5] Osman A., 2006. “Failure of a diesel engine injector nozzle by cavitation damage”, *Engineering Failure Analysis*, 2006(13), pp.11262-1133.

[6] Som S., Aggarwal S. K., EI-Hannouny E. M., et al., 2010. “Investigation of nozzle flow and cavitation characteristics in a diesel injector”. *ASME Journal of Engineering for Gas Turbines and Power*, 132, pp. 1-12.

[7] He Z.X., Li D.T., Hu L.F., et al., 2004. “Numerical simulation and analysis of two-phase flow of inner cavitation in injection nozzles”, *Transactions of CSICE (Chinese Society for Internal Combustion Engines)*, 22(5), pp. 433-438.

[8] He Z.X., Mu Q.M., Wang Q., et al., 2010. “Effect of diesel nozzle geometry on internal cavitating flow”, *Advanced Materials Research*, 97-101(2010),pp. 2925-2928.

[9] Rayleigh L., 1917. “On the pressure developed in a liquid during the collapse of a spherical cavity”, *Phil. Mag.* 34, pp. 94-98.

[10]Brennen C.E., 1995. Cavitation and bubble dynamics”, New York： Oxford University Press

[11]Guo L.J., 2002. Fluid dynamics of two phase and multiphase system, Xi'an: Xi'an Jiaotong University Press, (in Chinese).

[12]Tao W.Q., 1988. Numerical Heat Transfer, Xi'an: Xi'an Jiaotong University Press, (in Chinese).

[13]Nurick W.H.,1976. “Orifice cavitation and its effects on spray mixing”. *ASME J Fluids Eng* 68, pp.1-7.

[14]Arcoumanis C., Flora H., Gavalses M., et al., 2000. “Cavitation in real-size multi-hole diesel injector nozzles”, *SAE2000-01-1249*, pp. 1458-1499.

[15] Yuan W.X., Sauer J., Schnerr G. H., 2001. “Modeling and computation of unsteady cavitation flows in jnjection nozzles”, *Mec.Ind.*, 2, pp.383-394.

